Carbon 111 (2017) 182–190

Contents lists available at ScienceDirect

Carbon

journal homepage: www.elsevier.com/locate/carbon

Electric permittivity of reduced graphite oxide

Xinghua Hong [a, b], Weidong Yu [b], D.D.L. Chung [a, *]

[a] Composite Materials Research Laboratory, Department of Mechanical and Aerospace Engineering, University at Buffalo, The State University of New York, Buffalo, NY, 14260-4400, USA
[b] Key Laboratory of Textile Science & Technology, Ministry of Education, College of Textiles, Donghua University, Shanghai, 201620, China

ARTICLE INFO

Article history:
Received 24 August 2016
Received in revised form
26 September 2016
Accepted 27 September 2016
Available online 28 September 2016

ABSTRACT

The through-thickness electric permittivity (real part) of the solid part (53 vol%) of reduced graphite oxide (RGO) paper (100–300 μm thick, prepared by hydrazine reduction of modified-Hummers-method graphite oxide, GO) is 1130 (50 Hz), which is higher than that of the similarly tested parent GO (915, 50 Hz) and other carbons (31–124, 50 Hz). The high permittivity of RGO is attributed to the defects. Due to the conductivity of RGO, an insulating film between the specimen and an electrical contact is necessary during permittivity measurement using an RLC meter. Without the film, the measured capacitance is too high by 10–11 orders of magnitude, thus resulting in incorrectly high values of the permittivity. The relative permittivity 4×10^9 (20 Hz) reported by Sarkar et al. (2016) for similarly prepared RGO is therefore incorrect. The solid part of the RGO paper exhibits at 50 Hz in-plane conductivity 31 S/m, through-thickness conductivity 1.17 S/m, through-thickness relative permittivity (imaginary part) -4.2×10^8, through-thickness dielectric loss angle 90.0°, specific capacitance of the interface with an electrical contact 0.31 μF/m^2, and areal resistivity of this interface 0.18 Ω cm^2. The resistivity and specific capacitance of the RGO-contact interface are lower for RGO than GO.

1. Introduction

The real part of the relative electric permittivity (or relative dielectric constant) is a fundamental material property that describes the dielectric behavior of a material. This behavior relates to the polarizability. The permittivity is one of the key parameters that govern the electromagnetic and optical behavior of materials. Materials of high permittivity are needed for capacitors, ferroelectric memory, piezoelectric sensors and actuators, pyroelectric motion detectors and electromagnetic interference (EMI) shields.

Materials of high permittivity are mainly ceramics that are essentially non-conductive electrically. For example, $CaCu_3Ti_4O_{12}$ exhibits relative permittivity up to 3×10^5 at 1 kHz [1]. Carbon materials typically exhibit relatively low values of the relative permittivity (Table 1). Among the carbons listed, graphite oxide (GO) exhibits the highest relative permittivity of 915 at 50 Hz [2], with the polarizability stemming primarily from the functional groups. The relative permittivity of graphene is low, e.g., ~3 and ~1.8 in the through-thickness and in-plane directions respectively [3].

It has been recently reported that reduced graphite oxide (RGO) obtained by the reduction of GO using hydrazine exhibits relative permittivity 4×10^9 at 20 Hz [4]. This huge value (marking a phenomenon referred to as colossal dielectricity) is attributed to interfaces and defects [4]. This huge value calls for further research. Moreover, the prior work [4] reports the dielectric loss angle (δ) only for the frequency range (above 300 Hz) in which the relative permittivity approaches zero. In other words, the value of δ at the frequencies where the reported permittivity is high was not reported. Therefore, more complete characterization of the dielectric behavior of RGO is needed.

The dielectric behavior of polymer-matrix composites containing RGO as a filler is the subject of other prior work [5,6], which reports for the composites the permittivity values of 2080 at 1 kHz (12.5 vol% RGO) [5] and 350 at 1 kHz (3 wt% RGO) [6]. For epoxy containing 2 wt% exfoliated graphite, the relative permittivity has been reported to be 10^4 at 100 Hz [7]. For carbon fabric, the relative permittivity has been reported to be 4×10^6 at 10 Hz [8]. The values of 2080 [5], 10^4 [7] and 4×10^6 [8] are questionable also, as explained below.

The technique of permittivity measurement is critical to the reliability of the measured values. The technique commonly involves a precision RLC meter (for measuring the resistance *R*,

* Corresponding author.
E-mail address: ddlchung@buffalo.edu (D.D.L. Chung).
URL: http://alum.mit.edu/www/ddlchung

http://dx.doi.org/10.1016/j.carbon.2016.09.071
0008-6223/

Table 1
Relative permittivity of carbon materials at 50 Hz, all tested with the same method.

Material	Relative permittivity	Source
RGO	1130	This work
GO	915	[2]
Exfoliated graphite, not washed	360	[10]
Exfoliated graphite, washed with water	38	[9]
Natural graphite	53	[9]
Carbon black	31	[9]
Activated carbon	124	[9]
Activated graphite nanoplatelet	121	[9]

inductance L, and capacitance C), as is the case in the above-mentioned questionable prior work [4,5,7,8]. The meter works reliably in measuring the capacitance of electrically non-conductive materials. For conductive materials, the capacitance measurement provided by the meter can be severely inaccurate, e.g., higher than the true value by orders of magnitude, because the meter is not meant for measuring the capacitance of electrically conductive materials.

For measuring the capacitance of an electrically conductive material, a modified method has been developed [9,10]. In this method, the reliable measurement of the relative permittivity (real part) of a conductive material is made possible by (i) the presence of an electrically insulating polymer film at the interface between the specimen and each of the two electrical contacts, and (ii) the performance of the measurement at three (or more) specimen thicknesses and analyzing the data in terms of the slope of the plot of the reciprocal of the capacitance vs. the thickness. Step (ii) enables the decoupling of the contribution of the specimen-contact interface (with the contact including the film) to the measured capacitance from the contribution of the volume of the specimen, as the slope is inversely related to the relative permittivity (a volumetric property), while the intercept of the curve with the vertical axis at zero thickness relates to the interfacial capacitance (Fig. 1(a)). On the other hand, the film is obviously absent for the measurement of the conductivity. Similar conductivity measurement conducted at three (or more) specimen thicknesses enables the decoupling of the contribution of the specimen-contact interface to the measured resistance from the contribution of the volume of the specimen (Fig. 1(b)).

For the testing of RGO, as reported in this work, the removal of the insulating film in the capacitance measurement using an RLC meter increases the measured capacitance by orders of magnitude. Prior work on RGO [4], RGO composite [5], exfoliated graphite composite [7] and carbon fabric [8] uses the conventional method, which does not involve the insulating film.

This paper is aimed at (i) clarifying the previously reported huge value of the relative permittivity of RGO, (ii) establishing the technique of permittivity measurement of a conductive material using an RLC meter, (iii) providing a thorough characterization of the dielectric behavior of RGO, and (iv) providing a comparison of the dielectric behavior of RGO and the parent GO.

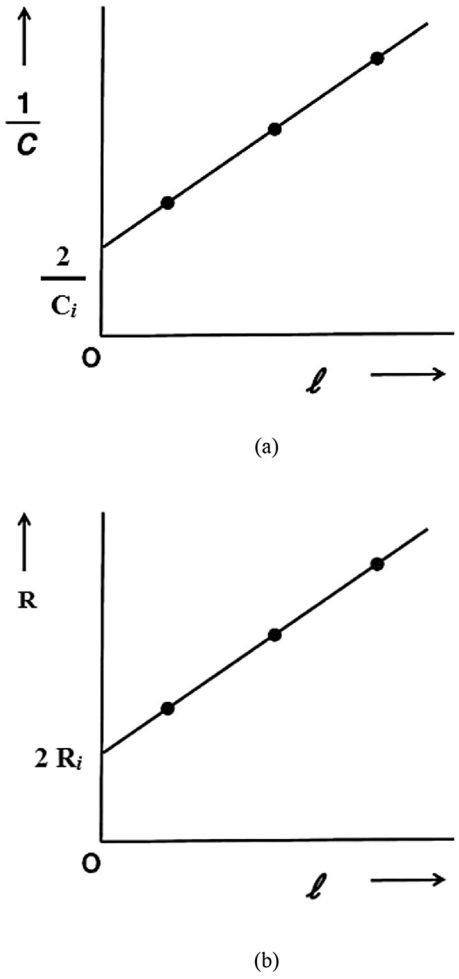

Fig. 1. (a) Schematic plot of $1/C$ vs. l, for the determination of C_i and κ based on Eq. (1). The slope equals $1/(\varepsilon_0 \kappa A)$, where κ is the relative permittivity of the specimen, ε_o is the permittivity of free space, l is the thickness of the specimen and A is the area of the specimen. The intercept on the vertical axis at $l = 0$ equals $2/C_i$. (b) Schematic plot of R vs. l for the determination of $\underline{R}_v$ and R_i based on Eq. (3). The slope equals the specimen resistance R_v per unit thickness. The intercept on the vertical axis equals two times R_i.

2. Experimental methods

2.1. Materials

The GO paper is prepared using the modified Hummers method [11], as in prior work on GO by these authors [2]. The RGO paper is obtained by the reduction of the GO paper. The reduction is performed at 105 °C for 6 h. The GO paper is supported by alumina such that it is above the top surface of the liquid, which is 2.0 g hydrazine hydrate in 100 mL de-ionized water. After reduction, the RGO paper is washed with de-ionized water and the excess water is removed by sandwiching the RGO paper with aluminum foils and squeezing out the water by manual compression of the sandwich. The process of washing and squeezing is repeated several times until the pH of the water reaches 7. The RGO paper is dried at 60 °C for 3 h immediately before testing. The volume fraction of solid in the RGO paper is (52.68 ± 0.25)%, as calculated based on the true density of RGO (2.200 g/cm^3 [12]).

The RGO that was reported in prior work [4] to exhibit a high permittivity of 4×10^9 at 20 Hz was prepared using essentially the same method as this work. As in this work, the modified Hummers method was used to prepare the GO, which was subsequently reduced to RGO by using hydrazine hydrate [4].

2.2. Testing methods

Unless noted otherwise, the reported results are for the through-thickness direction. For both through-thickness and in-plane electrical measurements, specimens at three thicknesses are tested. For the through-thickness testing, the specimen is a square of dimension 25.00 ± 0.10 mm at each edge of the square, as obtained by cutting, and the three thicknesses are

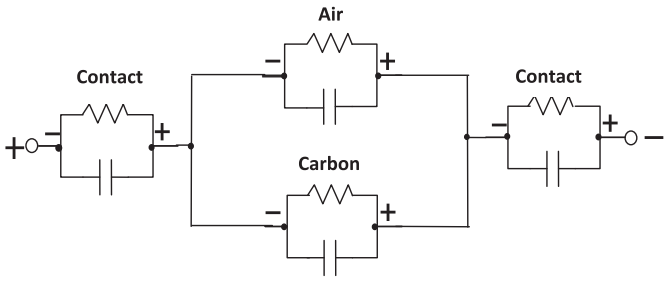

Fig. 2. Equivalent circuit model for the through-thickness electrical behavior of GO paper. The contact refers to the interface between the paper and an electrical contact.

0.100 ± 0.003 mm, 0.213 ± 0.003 mm and 0.303 ± 0.003 mm, which correspond to masses of 71.541 ± 0.001 mg, 153.112 ± 0.001 mg, 219.333 ± 0.001 mg, respectively. For the in-plane testing, the specimen is rectangular, of width 5.500 ± 0.003 mm, and the three thicknesses used are the same as those for the through-thickness testing.

The two-probe method is used for the through-thickness testing, whereas the four-probe method is used for the in-plane testing. The reliability of the two-probe method is enabled by the use of three thicknesses. For the in-plane testing, the two inner voltage probes are 19.200 ± 0.003 mm apart, while the two outer current probes are 25.000 ± 0.003 mm apart, with all four contacts being made with silver paint in conjunction with copper wires, such that each probe is around the entire perimeter in a plane perpendicular to the direction of resistance measurement. Please refer to our prior work [9,10] for the details in the testing set-up.

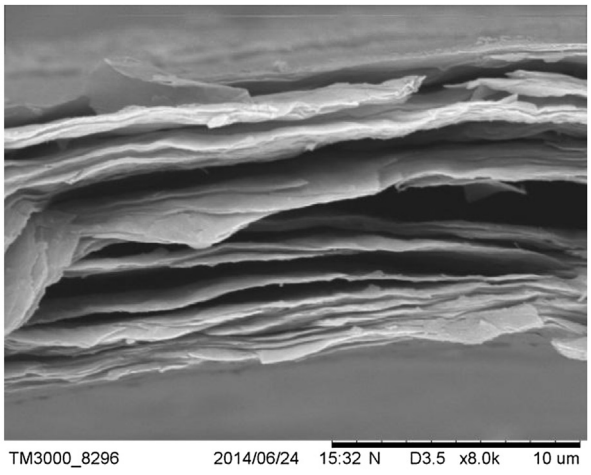

(a)

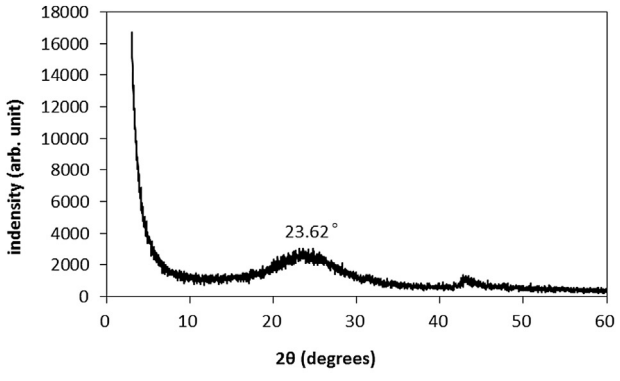

(b)

Fig. 3. Structure of the RGO paper. (a) SEM image of the cross-section. (b) XRD pattern.

The through-thickness relative permittivity (which describes the volumetric dielectric behavior of the RGO paper), the specific interfacial capacitance (which is the capacitance per unit area of the interface between the RGO paper and either electrical contact), the through-thickness electrical resistivity (which describes the geometry-independent through-thickness volumetric conduction behavior of the RGO paper) and the interfacial electrical resistivity (which is the geometry-independent areal resistivity of the interface between the RGO paper and either electrical contact) are measured in this work, using a precision RLC meter (Quadtech 7600), with the frequency ranging from 50 Hz to 2 MHz. The capacitance and resistance for the parallel RC circuit configuration are separately obtained from the meter, such that the capacitance is measured with an electrically insulating Teflon-coated glass fiber composite film (thickness 75 μm) between the RGO paper and each electrical contact, whereas the resistance is measured without this insulating film [2]. The AC voltage is adjusted so that the electric field is fixed at 22.6 V/cm while the thickness varies, so the voltage is 0.23, 0.48 and 0.68 V for the three thicknesses.

In order to decouple the volumetric and interfacial contributions to the capacitance, specimens of three different thicknesses are tested. In through-thickness testing, the electric field is applied between the two copper foils (thickness 62 μm), which serve as the electrical contacts. During through-thickness dielectric testing, a fixed pressure of 26.85 kPa is applied on the specimen in the direction perpendicular to the plane of the RGO paper. The decoupling of the contribution of the solid part of the RGO paper and the air contribution is performed by using the Rule of Mixtures, with solid RGO and air modeled as being electrically in parallel. Fig. 2 shows the equivalent circuit used in this work for modeling the conduction and dielectric behavior. In this circuit, carbon (the RGO solid in the paper) and air (the pores in the RGO paper) are electrically in parallel and this parallel combination is in series with both electrical contacts. In case of through-thickness measurement, these electrical contacts are in contact with the two opposite surfaces of the RGO paper, thereby sandwiching the paper. In case of in-plane measurement, the two electrical contacts are the inner voltage contacts on the specimen surface. In case of through-thickness measurement, all the quantities shown in the model are decoupled and determined using the method of prior work [9,10].

The volumetric capacitance of the RGO paper (C_v) and the capacitance of the interface between the paper and an electrical contact (C_i) are in series, so the measured capacitance C is given by

$$1/C = 2/C_i + 1/C_v \tag{1}$$

The factor of 2 in Eq. (1) is due to the presence of two interfaces on the two sides of the paper. Due to Eq. (1), C_i is less influential when it is large. The C_v is given by

$$C_v = \varepsilon_o \kappa A/l \tag{2}$$

where ε_o is the permittivity of free space (8.85×10^{-12} F/m), κ is the through-thickness relative permittivity (real part) of the RGO paper, A is the paper area (25.0×25.0 mm^2), and l is the paper thickness.

Due to Eqs. (1) and (2), the plot of $1/C$ against l is a straight line with the intercept of $2/C_i$ at the $1/C$ axis at $l = 0$, and the value of κ is

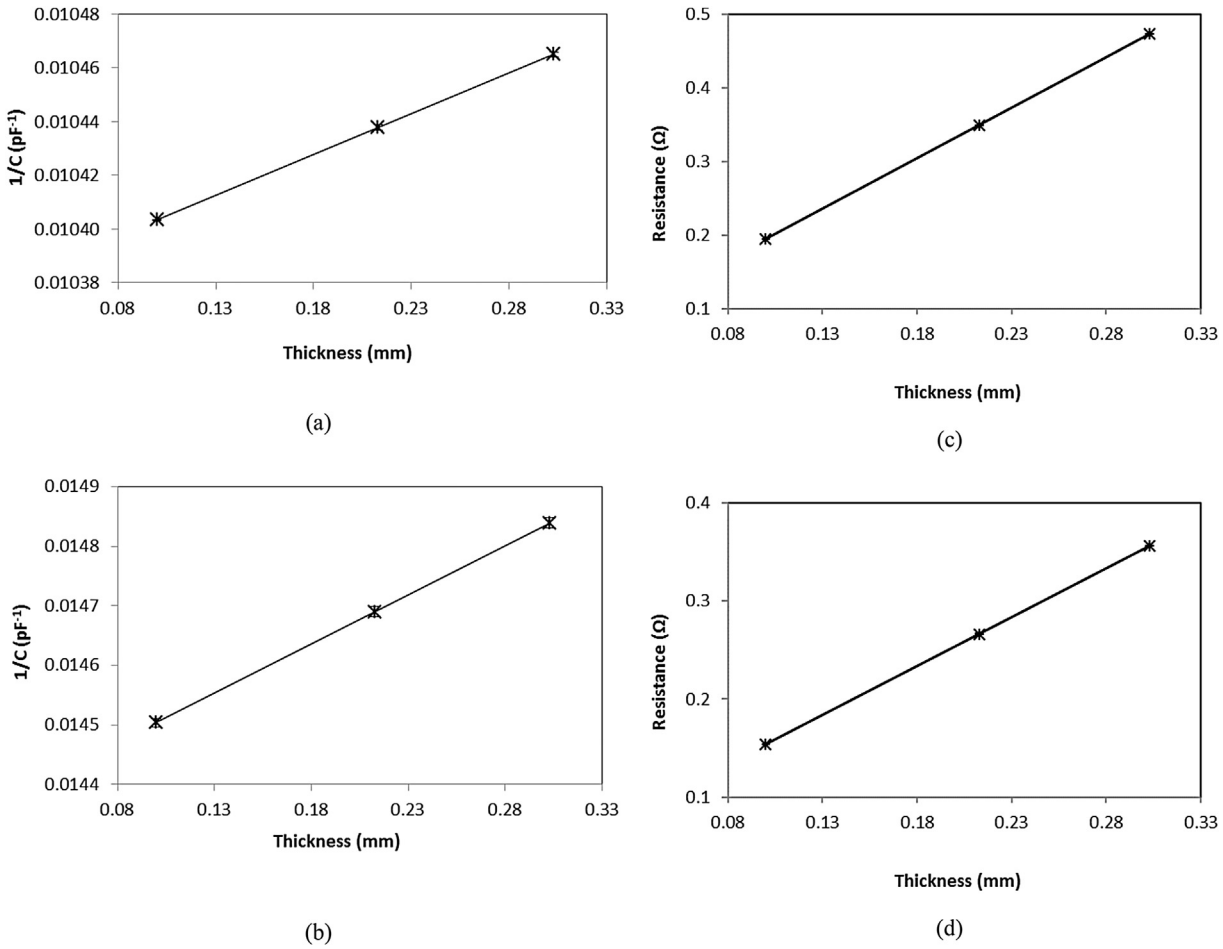

Fig. 4. (a–b) Plot of $1/C$ (where C is the measured capacitance, with an insulating film between the specimen and each electrical contact) vs. the RGO papers thickness (three different thicknesses) for the determination of the through-thickness permittivity. The error bars are shown, though they are too short to be clearly shown in (b). (a) 50 Hz. (b) 2 MHz. (c–d) Plot of the measured through-thickness resistance R vs. the specimen thickness for RGO papers of three different thicknesses. The error bars are shown, though they are too short to be shown clearly. (c) 50 Hz. (d) 2 MHz.

obtained from the slope, which is equal to $1/(\varepsilon_0 \kappa A)$. The specific interfacial capacitance for the overall paper is the product of C_i and A; that of the RGO in the paper is the product of C_i and the part of A that is occupied by the RGO (rather than air). The fraction of A that is occupied relates to the porosity of the paper and is taken as the volume fraction of solid in the paper.

The measured through-thickness resistance R between the two copper contacts that sandwich the paper in the absence of silver paint includes the through-thickness volume resistance R_v of the RGO paper and the resistance R_i of each of the two interfaces between the paper and a copper contact, i.e.,

$$R = R_v + 2R_i \tag{3}$$

By measuring R at three paper thicknesses, the curve of R versus thickness is obtained. The intercept of this curve with the R axis at zero thickness equals $2R_i$, whereas the slope of this curve equals R_v/l, where R_v is the paper resistance for the paper thickness of l. The through-thickness paper resistivity is obtained by multiplying R_v/l by the specimen area A. The paper conductivity is the inverse of the paper resistivity. The areal resistivity of the interface between the paper and an electrical contact equals the product of R_i and A; that of the interface between the RGO in the paper and an electrical contact equals the product of R_i and the part of A that is occupied by the RGO (rather than air).

For a conductive material, the conduction loss dominates the energy loss, so the imaginary part $-\kappa''$ (where κ'' is negative) of the relative permittivity is related to the conductivity σ by the equation

$$-\kappa'' = \sigma/(2\pi\nu\varepsilon_0) \tag{4}$$

where υ is the AC frequency. Eq. (4) is valid, at least approximately, due to the substantial conductivity of the RGO paper and the consequent dominance of the conduction contribution to the imaginary part of the relative permittivity.

The dielectric loss ($\tan\delta$) is obtained by using the equation

$$\tan\delta = -\kappa''/\kappa' = \sigma/(2\pi\nu\varepsilon_0\,\kappa'), \tag{5}$$

where κ' is the real part of the relative permittivity. For all the quantities, the decoupling of the contribution of the solid part of the paper and the air contribution is performed by using the Rule of Mixtures, with solid and air modeled as being electrically in parallel (Fig. 2) [10].

3. Results and discussion

3.1. Structure

The RGO paper is silver gray in color and is flexible. Fig. 3(a)

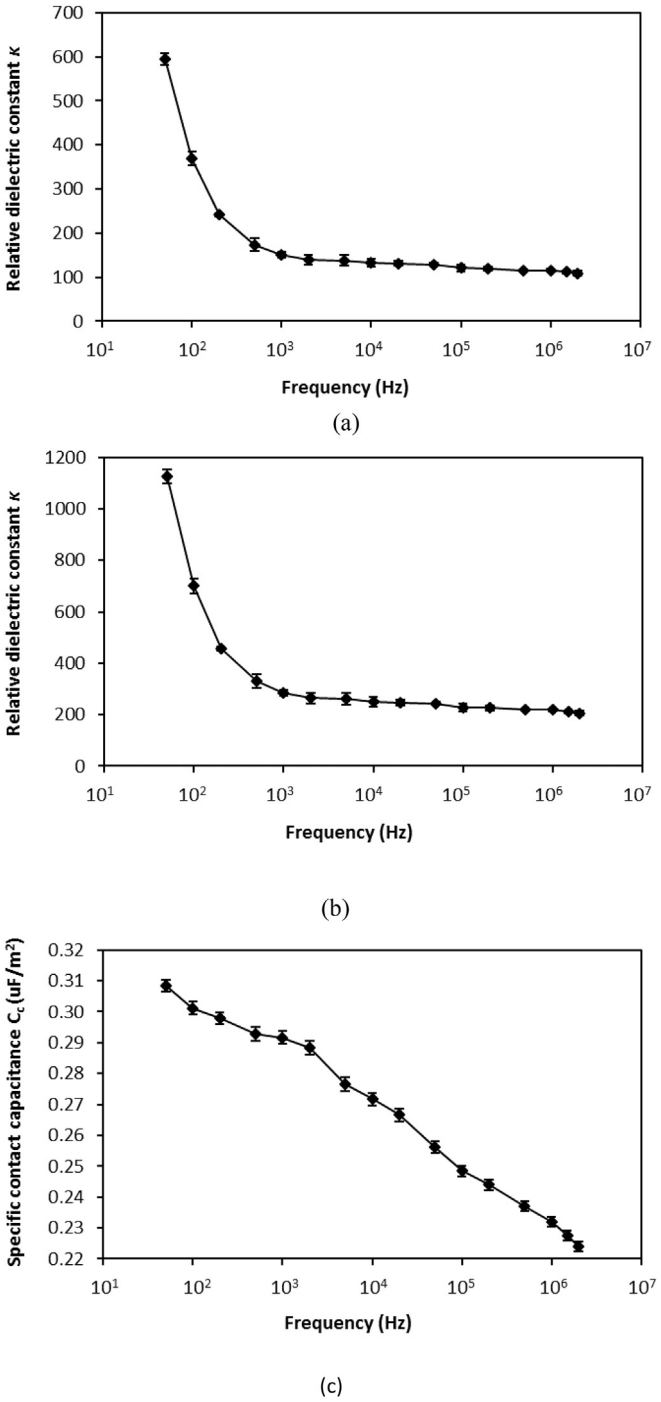

Fig. 5. Plot of the through-thickness relative permittivity (relative dielectric constant) κ of the RGO paper vs. the frequency. (a) The overall RGO paper (with air included). (b) The solid part of the RGO paper (with air excluded). (c) Plots of the through-thickness specific contact capacitance C_c between the solid part of the RGO paper and the electrical contact vs. the frequency.

shows the lamellar cross-sectional morphology of the RGO paper. It also shows substantial porosity, which is addressed in Sec. 2.1 through density measurement.

Fig. 3(b) shows the X-ray diffraction (XRD) pattern (obtained using CuKα radiation) of the RGO paper. The main peak is broad at $2\theta = 23.6^\circ$, which corresponds to an interlayer spacing of 3.77 Å. This peak position is downshifted from that of ideal graphite ($2\theta = 26^\circ$ which corresponds to an interlayer spacing of 3.42 Å). The downshift is typical for RGO [13,14]. In addition, there is a weak peak at $2\theta = 43^\circ$, which corresponds to an interlayer spacing of 2.10 Å. This weak peak is probably related to a combination of graphite 101 and graphite 100 [13,15]. Both the breadth of the main peak and the long tail below $2\theta = 10^\circ$ (previously reported for similarly prepared RGO [13]) indicate a degree of disorder in this carbon material.

The XRD pattern of the RGO that is reported in prior work [4] to exhibit a high permittivity of 4×10^9 at 20 Hz shows the main peak at $2\theta = 26^\circ$ (which is sharper than the main peak in Fig. 3(b)) and a minor peak at $2\theta = 44^\circ$, that is probably related to graphite 101 and graphite 100 (though it is labeled as graphite 100 in the prior work [4]), with the absence of the tail below $2\theta = 10^\circ$. Thus, the degree of order is higher in the RGO of the prior work [4] than the RGO of this work.

3.2. Dielectric and electrical behavior

Fig. 4 shows representative plots of the reciprocal of the capacitance vs. RGO paper thickness and of the resistance vs. paper thickness. The strong linearity of all the plots in Fig. 4 is consistent with Eqs. (1) and (3) and supports the validity of this work's approach for decoupling of the volumetric and interfacial contributions.

Fig. 5(a) and (b) show the through-thickness relative permittivity. The highest value is 595 for the RGO paper (with air included) and 1130 for the solid part of the paper (with air excluded), both obtained at the lowest frequency of 50 Hz. At the highest frequency (2 MHz) studied, the solid part of the paper exhibits relative permittivity 206 only (Fig. 5(b)). These values are all higher than those of similarly tested parent GO paper [2] and are attributed to defects [16–18] and the functional groups (e.g., oxygen-containing functional groups) [18–20] associated with the defects. Defects are abundant in RGO due to the removal of some of the carbon atoms during the oxygen atom removal in the reduction process. For graphene, the relative permittivity is very low (e.g., 3) [3], due the low amount of defects. The Fourier-transform infrared (FTIR) spectrum in Fig. 6 shows the functional groups in the RGO and the parent GO. The amount of functional groups is less for RGO than GO, but the C-O groups are substantial for RGO.

Table 1 compares the relative permittivity (50 Hz) of the RGO of this work and various carbon materials of prior work [2,9,10]. Among all the carbons, RGO exhibits the highest value of the relative permittivity.

The through-thickness relative permittivity decreases with increasing frequency, as expected. The decrease is particularly abrupt in the low frequency regime from 50 Hz to 1 kHz. Above 1 kHz, the relative permittivity essentially levels off (at a value around 220 for the RGO solid) up to the highest frequency of 2 MHz. The trend is the same for both the overall paper (with air included) and the solid part of the paper (with air excluded). This trend is attributed to the dipole friction associated with the functional groups on the RGO.

Fig. 5(c) shows that the specific contact capacitance of the RGO-contact interface (where RGO refers to the solid part of the paper) decreases steadily with increasing frequency. The values range from 0.31 $\mu F/m^2$ at the lowest frequency of 50 Hz to 0.22 $\mu F/m^2$ at the highest frequency of 2 MHz. These values are much lower than those of the parent GO paper [2]. In view of Eq. (1), this means that the interface for RGO influences the measured capacitance more than the corresponding interface for the parent GO.

Fig. 7(a) shows that the through-thickness AC conductivity of the solid part of the RGO paper increases with increasing frequency, such that the increase is more significant at frequencies above 1 MHz than frequencies below 1 MHz. The conductivity ranges

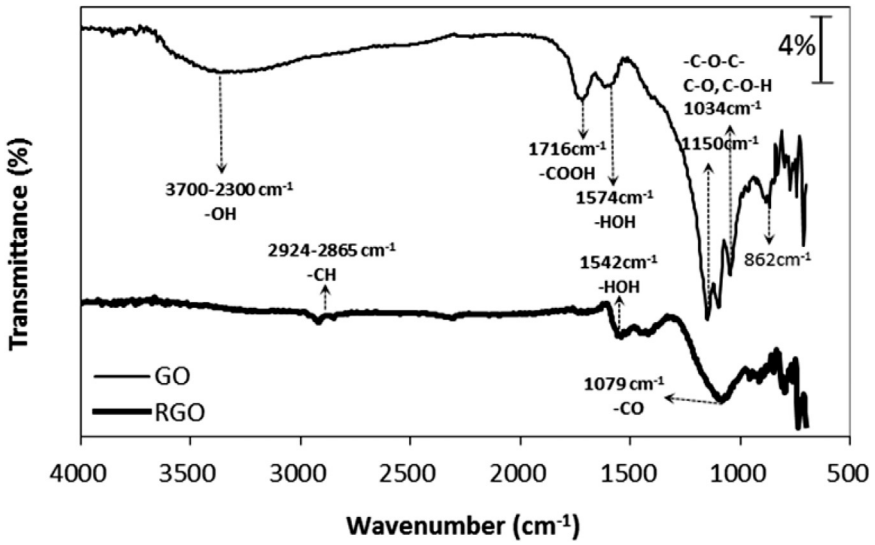

Fig. 6. FTIR spectra of RGO and the parent GO.

from 1.17 S/m at the lowest frequency of 50 Hz to 1.61 S/m at the highest frequency of 2 MHz. These values are higher than those of the parent GO paper [2] by 3–6 orders of magnitude. However, they are lower than those of exfoliated graphite [10] by 1 order of magnitude. The higher conductivity of exfoliated graphite is attributed to the connectivity resulting from the mechanical

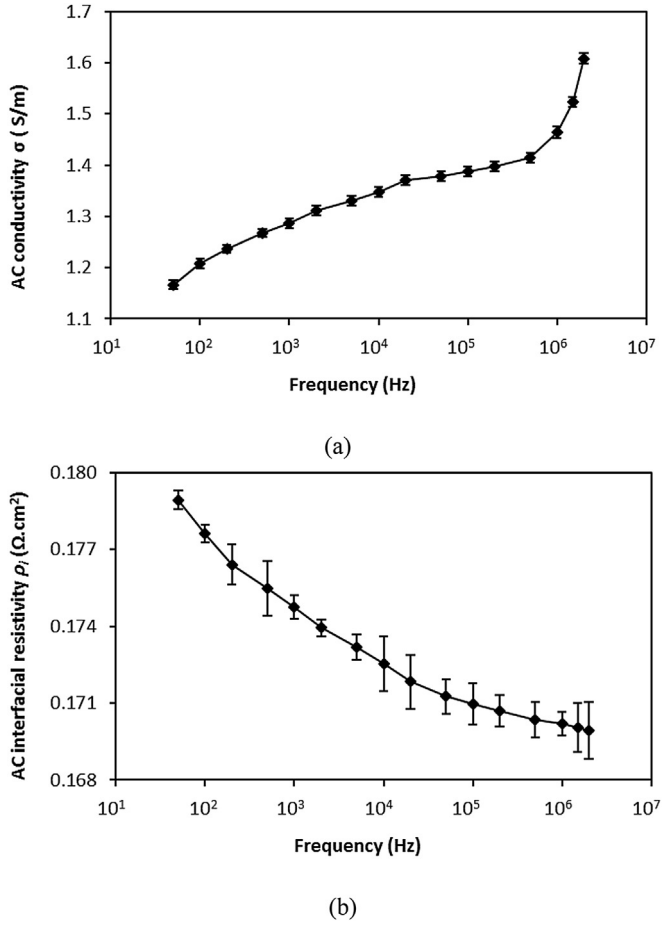

Fig. 7. (a) Plots of the through-thickness volume electrical conductivity σ of the solid part of the RGO paper vs. the frequency. (b) Plots of the interfacial resistivity ρ_i between the solid part of the RGO paper and an electrical contact vs. the frequency. The error bars in (a) are present, but they are too short to be shown clearly.

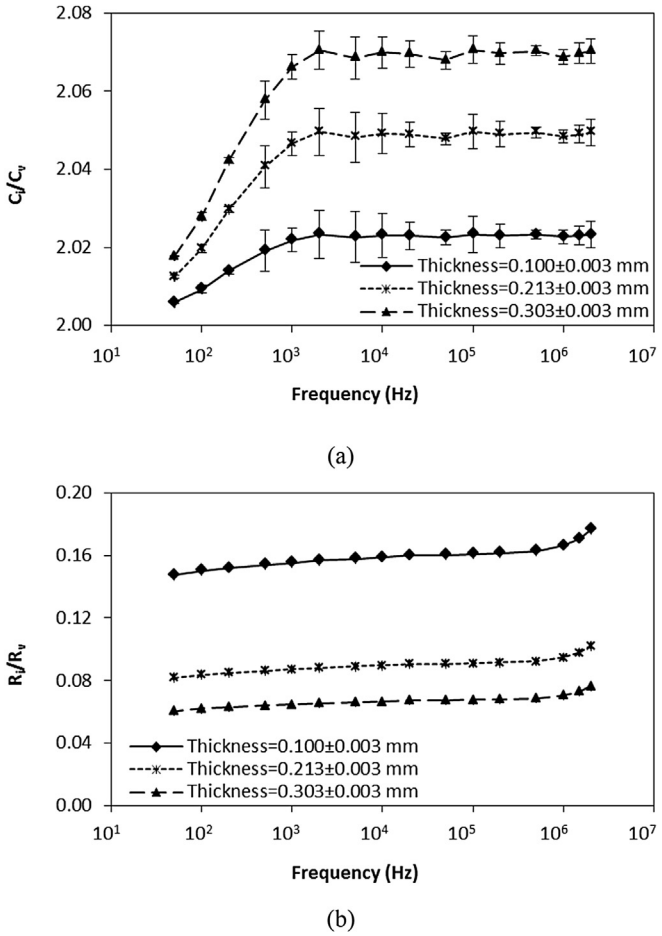

Fig. 8. The ratio of the contribution of the interface between the specimen and the electrical contact to the contribution of the volume of the specimen. (a) Capacitance. (b) Resistance.

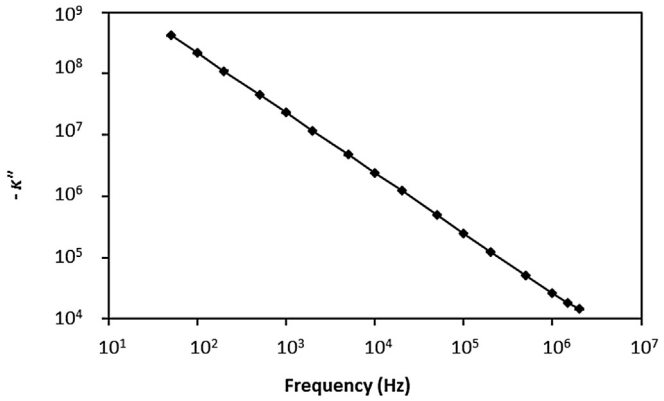

Fig. 9. Plots of the negative of the imaginary part of the through-thickness relative permittivity κ'' (logarithmic scale) of the solid part of the RGO paper vs. the frequency (logarithmic scale). The term "solid" refers to the solid part of the material, with the air excluded.

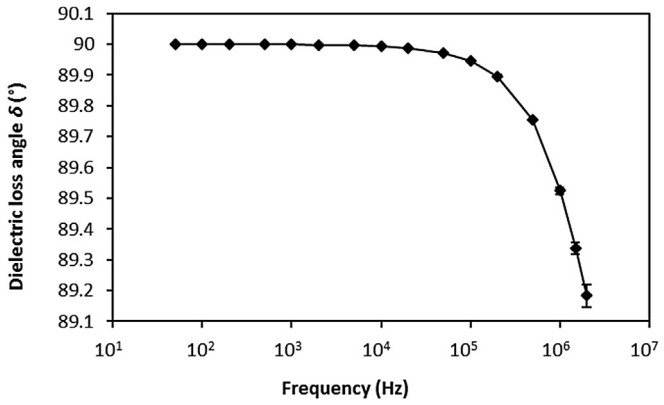

Fig. 10. Plots of the through-thickness dielectric loss angle δ of the solid part of the RGO paper vs. the frequency.

interlocking that is enabled by the cellular structure of exfoliated graphite [21].

The abovementioned frequency dependence of the through-thickness conductivity is attributed to the decreasing excursion of the charge carriers in a cycle as the frequency increases and the consequent decrease in the chance of the carriers to encounter an interface, such as the interface between adjacent RGO flakes (with each flake being essentially a stack of a few carbon layers). Since the relevant conductivity is in the through-thickness direction of the RGO paper, there are numerous inter-flake interfaces along the thickness of the paper and the carriers can encounter these interfaces as they move in response to the applied electric field. Due to the relatively high resistance at each of these interfaces, the less that the carriers encounter interfaces, the greater is the conductivity.

Fig. 7(b) shows the areal resistivity of the interface between the solid part of the RGO paper and an electrical contact. This resistivity decreases steadily with increasing frequency. In general, the resistivity of an interface tends to be lower when the materials of the proximate surfaces that come together to form this interface are more conductive. Therefore, the trend of the interfacial resistivity in Fig. 7(b) is consistent with the trend of the volumetric conductivity in Fig. 7(a). The interfacial resistivity of the solid part of the RGO paper ranges from 0.179 Ω cm^2 at the lowest frequency of 50 Hz to 0.170 Ω cm^2 at the highest frequency of 2 MHz. These values are lower than those of the parent GO paper [2] by 3–6 orders of magnitude.

Fig. 8(a) shows that, for the paper dimensions of this work, C_i is higher than C_v by a factor of 2.0–2.1, meaning that the volumetric capacitance contributes substantially to the measured capacitance, though the interfacial capacitance dominates. The ratio of C_i to C_v is essentially independent of the frequency above 1 kHz. The greater is the thickness, the higher is the ratio. This is because a greater thickness is associated with a lower volumetric capacitance. Compared to the parent GO paper [2], this ratio is smaller, due to the higher permittivity.

Fig. 8(b) shows that, for the RGO paper dimensions of this work, the ratio of R_i to R_v is below 0.2, meaning that R_i contributes to the measured resistance, though R_v dominates. The ratio is quite independent of the frequency up to 1 MHz. The smaller is the thickness, the greater is the ratio. This is because a smaller thickness is associated with a lower through-thickness volumetric resistance.

Fig. 9 shows that the log-log plot of the frequency dependence of the negative of the imaginary part of the relative permittivity κ''. This plot is linear up to the highest frequency of 2 MHz. The linearity is consistent with Eq. (4). The value of $-\kappa''$ ranges from 4.20×10^8 at the lowest frequency of 50 Hz to 1.45×10^4 at the highest frequency of 2 MHz. These values are much lower than the values ranging from 10^{11} at the same lowest frequency to 10^6 at the same highest frequency for exfoliated graphite that has not been washed [10], as expected due to the lower conductivity of RGO compared to the exfoliated graphite.

Fig. 10 shows that the dielectric loss angle δ is quite high. It decreases with increasing frequency, ranging from 90.0° at 50 Hz to 89.2° at 2 MHz, such that the decrease mostly occurs above 100 kHz. The high value of δ is consistent with the substantial conductivity, which is attractive for electrode applications. High loss is also attractive for electromagnetic interference (EMI) shielding, although the frequencies used in this study are low compared to the typical frequencies (such as 1 GHz) used for EMI shielding. High loss is not desirable for the dielectric material in a dielectric capacitor, but this is not an intended application of RGO. Even higher values of the loss angle have been previously reported for exfoliated graphite that has not been washed with water to remove the residual acidity [10].

The in-plane conductivity of the solid part of the RGO paper (Fig. 11(a)) increases with increasing frequency. It increases slightly with decreasing thickness, due to the increasing preferred orientation of the carbon layers as the thickness decreases. The increase with increasing frequency is less severe for the in-plane conductivity than the through-thickness conductivity (Fig. 7(a)). This is attributed to the difference in the effect of the interfaces in the material. The interface effect is small in the in-plane direction compared to that in the through-thickness direction, as expected from the preferred orientation of the carbon layers in the plane of the paper.

As shown in Fig. 11(a), the highest in-plane conductivity obtained for the solid part of the paper is 204 S/m, which is higher than the corresponding value of 2.5 S/m for the parent GO paper. Fig. 11(b) shows that the ratio of the in-plane conductivity to through-thickness conductivity (both for the solid part of the RGO paper) increases with increasing frequency. This means that the degree of electrical anisotropy increases with increasing frequency.

Fig. 11(c) and (d) show that both the ratio of the through-thickness conductivity of the solid part of the RGO paper to that of the GO paper and the ratio of the in-plane conductivity of the solid part of the RGO paper to that of the parent GO paper are much greater than 1, indicating that the through-thickness conductivity is higher for RGO than the parent GO. The frequency dependence shown in Fig. 11(c) and (d) indicates that the through-thickness or

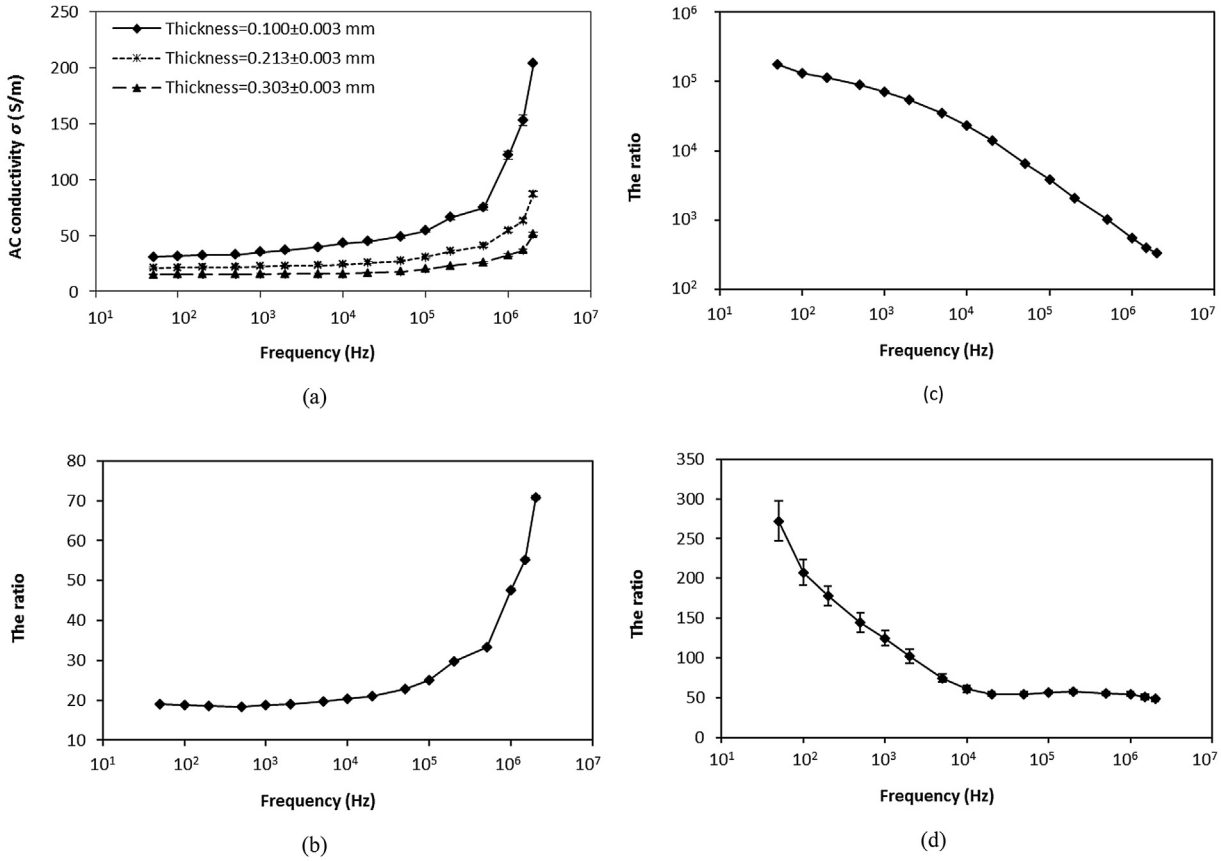

Fig. 11. (a) Plot of the in-plane conductivity of the solid part of the RGO paper vs. the frequency, showing the effect of the paper thickness on the conductivity. (b) The ratio of in-plane conductivity to through-thickness conductivity of the solid part of the RGO paper vs. the frequency. The in-plane values are the average of those of three thicknesses. (c) The ratio of through-thickness conductivity of the solid part of the RGO paper to through-thickness conductivity of the solid part of the GO paper vs. the frequency. (d) The ratio of in-plane conductivity of the solid part of the RGO paper to in-plane conductivity of the solid part of the GO paper vs. the frequency. The in-plane values are the average of those of three thicknesses.

Table 2
Comparison of the capacitance and permittivity results of RGO obtained with and without an insulating film between the specimen and each of the two electrical contacts.

	With insulating film	Without insulating film
Capacitance (pF), thickness 0.100 ± 0.003 mm	96.1235 ± 0.0014	$1.15 \times 10^{12} \pm 1.01 \times 10^{10}$
Capacitance (pF), thickness 0.213 ± 0.003 mm	95.8072 ± 0.0099	$5.69 \times 10^{11} \pm 3.93 \times 10^{9}$
Capacitance (pF), thickness 0.303 ± 0.003 mm	95.5568 ± 0.0081	$3.97 \times 10^{11} \pm 2.83 \times 10^{9}$
Relative permittivity of RGO paper	594.7 ± 14.2	$2.24 \times 10^{10} \pm 1.34 \times 10^{8}$
Relative permittivity of the solid part of the RGO paper	1128 ± 27	$4.25 \times 10^{10} \pm 2.54 \times 10^{8}$

in-plane electrical conductivity of RGO and that of the parent GO become closer as the frequency increases, probably because the chance of the carriers to encounter defects (which differ between RGO and GO) decreases as the carrier excursion in a cycle decreases.

Prior work that reported relative permittivity 4×10^9 at 20 Hz [4] for RGO attributed the high permittivity to interfaces and defects. As indicated by XRD, the RGO of this work is less ordered than that of prior work [4]. In spite of the lower degree of order, the RGO of this work gives a much lower permittivity of 1130 (50 Hz).

The testing method of this work and prior work [4] involves similar RLC meters, but the details of the method differ. This work uses an insulating film between the specimen and each of the two electrical contacts, whereas the prior work [4] apparently did not. As shown in this work by testing the permittivity of the RGO with and without the insulating film, the measured capacitance is higher by orders of magnitude (reaching unreasonably high values) when the film is absent (Table 2 and Fig. 12). Without the insulating film, the measured capacitance is too high by 10–11 orders of magnitude, thus resulting in incorrectly high values of the relative permittivity. Therefore, it is clear that the huge permittivity of the prior work [4] is incorrect. The correct value found in this work is 1130 at 50 Hz, which is close to the frequency of 20 Hz of prior work [4].

The electrical conductivity of the RGO of prior work is 1000 S/m [4], which is much higher than both the in-plane and through-thickness conductivity of this work. The higher conductivity of the RGO of the prior work is consistent with the higher degree of order shown by XRD. The high conductivity aggravates the permittivity measurement problem mentioned above.

The permittivity value of 2080 at 1 kHz reported for a polymer-matrix composite containing 12.5 vol% RGO [5] was also obtained without the use of an insulating film. Therefore, this reported value

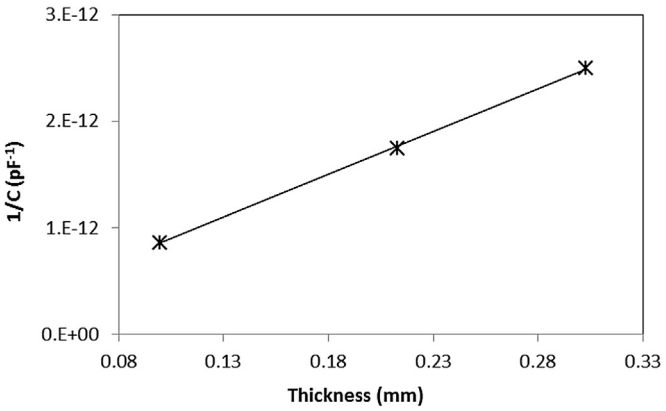

Fig. 12. Plot of 1/*C* (50 Hz, where *C* is the measured capacitance, without an insulating film between the specimen and each electrical contact) vs. the RGO paper thickness (three different thicknesses) for the determination of the through-thickness relative permittivity. The error bars are shown, though they are too short to be clearly shown.

is likely to be much higher than the true value.

As shown in Table 1, the relative permittivity of the RGO is higher than the values for previously reported carbon materials, in spite of its relatively high conductivity. The combination of high permittivity and high conductivity is attractive for applications that benefit from the ability of the carbon material to polarize while it is conductive. An example is a polarizable electrode.

4. Conclusions

The through-thickness electric permittivity of the solid part (53 vol%) of hydrazine-reduced RGO paper (100–300 μm thick) is 1130 and 200 at 50 Hz and 2 MHz respectively. The values are higher than those previously reported for similarly tested parent GO [2], exfoliated graphite (whether washed or not washed with water) [9,10], natural graphite [9], carbon black [9], activated carbon [9] and activated graphite nanoplatelet [9]. The high permittivity of RGO is attributed to the defects and the associated functional groups.

The previously reported relative permittivity of 4×10^9 (20 Hz) [4] for similarly prepared RGO is incorrect. The correct value is 1130 (50 Hz). Due to the conductivity of RGO, it is necessary to use an insulating film between the specimen and the electrical contact during the measurement of the permittivity using an RLC meter. Without the insulating film, the measured capacitance is too high by 10–11 orders of magnitude, thus resulting in incorrectly high values of the relative permittivity.

The solid part of the RGO paper exhibits, at 50 Hz and 2 MHz respectively, in-plane conductivity 31 and 204 S/m, through-thickness conductivity 1.17 and 1.61 S/m, through-thickness relative permittivity (imaginary part) -4.2×10^8 and -1.4×10^4, through-thickness dielectric loss angle 90.0° and 89.2°, specific capacitance of the interface with an electrical contact 0.31 and 0.22 μF/m^2, and areal resistivity of this interface 0.18 and 0.17 Ω cm^2.

The relative permittivity (real part) of 1130 is higher than the value of 915 for the parent GO, due to the defects and associated functional groups in RGO. Both in-plane conductivity and through-thickness conductivity are much higher than those of GO. The specific capacitance of the interface with an electrical contact is lower than that of GO. The areal resistivity of this interface is much lower than that of GO.

References

[1] S. Guillemet-Fritsch, T. Lebey, M. Boulos, B. Durand, Dielectric properties of CaCu3Ti4O12 based multiphased ceramics, J. Eur. Ceram. Soc. 26 (2006) 1245–1257.
[2] X. Hong, W. Yu, A. Wang, D.D.L. Chung, Graphite oxide paper as a polarizable electrical conductor in the through-thickness direction, Carbon (2016) (in press).
[3] E.J.G. Santos, E. Kaxiras, Electric-field dependence of the effective dielectric constant in graphene, Nano Lett. 13 (2013) 898–902.
[4] S. Sarkar, A. Mondal, K. Dey, R. Ray, Defect driven tailoring of colossal dielectricity of reduced graphene oxide, Mater. Res. Bull. 74 (2016) 465–471.
[5] L. Cui, X. Lu, D. Chao, H. Liu, Y. Li, C. Wang, Graphene-based composite materials with high dielectric permittivity via an in situ reduction method, Phys. Status Solidi A 208 (2) (2011) 459–461.
[6] T. Chen, J. Qiu, K. Zhu, J. Li, J. Wang, S. Li, X. Wang, Ultra high permittivity and significantly enhanced electric field induced strain in PEDOT: PSS–RGO@PU intelligent shape-changing electro-active polymers, RSC Adv. 4 (2014) 64061–64067.
[7] I. Kranauskaite, J. Macutkevic, P. Kuzhir, N. Volynets, A. Paddubskaya, D. Bychanok, S. Maksimenko, J. Banys, R. Juskenas, S. Bistarelli, A. Cataldo, F. Micciulla, S. Bellucci, V. Fierro, A. Celzard, Dielectric properties of graphite-based epoxy composites, Phys. Status Solidi A 211 (7) (2014) 1623–1633.
[8] B. Qiu, J. Guo, Y. Wang, X. Wei, Q. Wang, D. Sun, M.A. Khan, D.P. Young, R. O'Connor, X. Huang, X. Zhang, B.L. Weeks, S. Wei, Z. Guo, Dielectric properties and magnetoresistance behavior of polyaniline coated carbon fabrics, J. Mater. Chem. C 3 (2015) 3989–3998.
[9] A. Wang, D.D.L. Chung, Dielectric and electrical conduction behavior of carbon paste electrochemical electrodes, with decoupling of carbon, electrolyte and interface contributions, Carbon 72 (2014) 135–151.
[10] X. Hong, D.D.L. Chung, Exfoliated graphite with relative dielectric constant reaching 360, obtained by exfoliation of acid-intercalated graphite flakes without subsequent removal of the residual acidity, Carbon 91 (2015) 1–10.
[11] W.S. Hummers Jr., R.E. Offeman, Preparation of graphitic oxide, J. Am. Chem. Soc. 80 (6) (1958), 1339–1339.
[12] S. Tankovich, D.A. Dikin, R.D. Piner, K.A. Kohlhaas, A. Kleinhammes, Y. Jia, R.S. Ruoff, Synthesis of graphene-based nanosheets via chemical reduction of exfoliated graphite oxide, Carbon 45 (7) (2007) 1558–1565.
[13] S. Park, J. An, J.R. Potts, A. Velamakanni, S. Murali, R.S. Ruoff, Hydrazine-reduction of graphite- and graphene oxide, Carbon 49 (2011) 3019–3023.
[14] H. Chen, M.B. Muller, K.J. Gilmore, G.G. Wallace, D. Li, Mechanically strong, electrically conductive, and biocompatible graphene paper, Adv. Mater. 20 (2008) 3557–3561.
[15] G. Wang, J. Yang, J. Park, X. Gou, B. Wang, H. Liu, J. Yao, Facile synthesis and characterization of graphene nanosheets, J. Phys. Chem. C 112 (2008) 8192–8195.
[16] Matsumoto M, Saito Y, Park C, Fukushima T, Aida T. Ultrahigh-throughput exfoliation of graphite into pristine 'single-layer' graphene using microwaves and molecularly engineered ionic liquids. Nat. Chem. 7(9):730–736.
[17] L. Chen, J. Lei, F. Wang, G. Wang, H. Feng, Facile synthesis of graphene sheets from fluorinated graphite, RSC Adv. 5 (50) (2015) 40148–40153.
[18] Yang Hu, Shaoxian Song, Alejandro Lopez-Valdivieso, Effects of oxidation on the defect of reduced graphene oxides in graphene preparation, J. Colloid Interface Sci. 450 (2015) 68–73.
[19] Y. Guo, X. Sun, Y. Liu, W. Wang, H. Qiu, J. Gao, One pot preparation of reduced graphene oxide (RGO) or Au (Ag) nanoparticle-RGO hybrids using chitosan as a reducing and stabilizing agent and their use in methanol electrooxidation, Carbon 50 (2012) 2513–2523.
[20] H.S. Song, M.G. Park, W. Ahn, S.N. Lim, K.B. Yi, E. Croiset, Z. Chen, S.C. Nam, Enhanced adsorption of hydrogen sulfide and regeneration ability on the composites of zinc oxide with reduced graphite oxide, Chem. Eng. J. Amst. Neth. 253 (2014) 264–273.
[21] D.D.L. Chung, A review of exfoliated graphite, J. Mater. Sci. 51 (2016) 554–568.